Published in final edited form as:
J Immunol. 2014 July 15; 193(2): 564–570. doi:10.4049/jimmunol.1400825.

Site-specific chemokine expression regulates CNS inflammation and determines clinical phenotype in autoimmune encephalomyelitis[1]

Joshua S. Stoolman[*,†], **Patrick C. Duncker**[*,†], **Amanda K. Huber**[*], and **Benjamin M. Segal**[*,†,‡]

[*]Holtom-Garrett Program in Neuroimmunology & Multiple Sclerosis Center, Department of Neurology, University of Michigan School of Medicine, Ann Arbor, MI 48109.

[†]Graduate Program in Immunology, University of Michigan School of Medicine, Ann Arbor, MI 48109.

[‡]Neuroscience Program, University of Michigan School of Medicine, Ann Arbor, MI 48109.

Abstract

The adoptive transfer of myelin-reactive T cells into wildtype (WT)[2] hosts results in spinal cord inflammation and ascending paralysis, referred to as conventional experimental autoutoimmune encephalitis (EAE)[3], as opposed to brainstem inflammation and ataxia, which characterize disease in IFNγRKO hosts (atypical EAE). Here we show that atypical EAE correlates with preferential upregulation of CXCL2 in the brainstem, and is driven by CXCR2 dependent recruitment of neutrophils. In contrast, conventional EAE is associated with upregulation of CCL2 in the spinal cord, and is driven by recruitment of monocytes via a partially CCR2-dependent pathway. This study illustrates how regional differences in chemokine expression within a target organ shape the spatial pattern and composition of autoimmune infiltrates, leading to disparate clinical outcomes.

Introduction

A defining feature of multiple sclerosis (MS)[4] is the spatial dissemination of inflammatory demyelinating lesions within the CNS (1). In some patients, lesion burden is concentrated in the spinal cord with little involvement of the cerebrum (as in the opticospinal form of disease that is more common in Asia, or in a significant cohort of individuals with primary progressive MS) (2–4). In others, lesion burden is skewed supratentorially, with little to no involvement of the spinal cord (as in a significant cohort of individuals with relapsing

[1]This research was supported by the US National Institutes of Health (NINDS R01 NS057670 to B.M.S.).

[2]Wild Type (WT)

[3]Experimental Autoimmune Encephalomyelitis (EAE)

Address correspondence and reprint request to Dr. Benjamin M. Segal, Department of Neurology, 4013 BSRB, 109 Zina Pitcher Place, Ann Arbor, MI 48109. Tel: 734-615-5635; Fax: 734-615-7300; bmsegal@umich.edu.

Disclosure
The authors have no financial conflicts of interest.

[4]Multiple Sclerosis (MS)

remitting MS in the Western Hemisphere) (5, 6). The factors that regulate leukocyte trafficking to, and accumulation in, particular regions of the CNS are poorly understood.

EAE, widely used as an animal model of MS, classically manifests as an ascending paralysis that correlates with inflammatory demyelination of the lumbosacral spinal cord (7). In certain instances, an atypical form of EAE has been observed in which afflicted mice exhibit signs of imbalance/ vestibular dysfunction that correlate with lesion formation in the brainstem and/ or cerebellar white matter (8–13). This clinical phenotype occurs most consistently and prominently under circumstances where IFNγ bioactivity is suppressed. Hence, IFNγ- and IFNγ receptor (IFNγR)[5]-deficient mice are significantly more likely to develop atypical EAE than their WT counterparts following active immunization (10). Adoptive transfer experiments have demonstrated that either deficient IFNγ production by encephalitogenic donor T cells or impaired IFNγ signaling into host cells is sufficient for the development of atypical EAE (12–14).

In some experimental paradigms, a high incidence of atypical disease has been observed following the transfer of encephalitogenic T cell lines that contain a high ratio of Th17 to Th1 cells. In contrast, conventional disease is mediated by T cell lines that express a low Th17:Th1 ratio (11). A major function of IL-17, the signature Th17 cytokine, is to induce neutrophil mobilizing/activating factors, such as G-CSF, and chemokines that target granulocytes, such as CXCL1, CXCL2 and CXCL5 (15). Conversely, IFNγ skews myeloid cell differentiation in the bone marrow to favor monocytes over granulocytes during immune activation (16). Therefore, it is not surprising that atypical disease tends to be characterized by neutrophil-rich white matter infiltrates, while monocytes are more prevalent in the infiltrates of mice with conventional disease (10, 13, 14). However, a distinctive requirement for neutrophil mobilizing/ activating factors in atypical EAE versus monocyte mobilizing factors in conventional EAE has yet to be directly demonstrated.

In the current paper we compared atypical and conventional EAE, induced in IFNγRKO and WT hosts, respectively, by transfer of the same population of myelin oligodendrocyte (MOG)[6] peptide-primed, IL-12 polarized $CD4^+$ T cells. We found that atypical EAE correlates with preferential upregulation of CXCL2 in the brainstem of IFNγRKO hosts, and is driven by CXCR2-dependent recruitment of neutrophils to the white matter tracts surrounding the vestibulocochlear nucleus (VCO)[7]. In WT mice, that have an intact IFNγ signaling pathway, brainstem CXCL2 expression is suppressed and spinal cord CCL2 is upregulated. Consequently, the autoimmune assault is redirected to the spinal cord and manifests as a monocyte-predominant infiltrate that is, in part, CCR2 dependent.

Materials and Methods

Mice

8- to 14 week old CD45.1 congenic and WT C57BL/6 mice were obtained from NCI Fredrick or Jackson Laboratory. IFNγR knock-out (KO) (B6.129S7-*Ifngr1*^{tm1Agt}/J)[8] and

[5]Interferon-γ receptor (IFNγR)
[6]Myelin Oligodendrocyte Glycoprotein (MOG)
[7]Vestibulocochlear Nucleus (VCO)

IFNγKO (B6.129S7-*Ifng*^{tm1Ts}/J) mice were obtained from Jackson Laboratory. Breeding pairs of IL-17RKO originally obtained from from J. Kolls (LSU) and CCR2KO mice from B. Moore (University of Michigan) were bred in our facility. Mice were housed in microisolator cages under specific pathogen-free conditions. All animal protocols were approved by the University Committee on Use and Care of Animals.

Antibodies and Reagents

Rat antibody to myelin basic protein (MBP)[9] (clone 12) was from Millipore. Mouse antibody to unphosphorylated filament –H (SMI)[10] was from Covance. AlexaFluor594 goat-anti-mouse IgG and AlexaFluor488 goat-anti-rat IgG were from Life Technologies. The following antibodies were obtained from ebiosciences: FITC-anti-MHCII (M5/114.15.12), FITC-anti-B220 (RA3-6132), PE-anti-CD45 (Ly5), PE-anti-CD8α (53-6.7), PE-anti-CD4 (Gk1.5), PE-anti-GM-CSF (MP1-22E9), PECy7-anti-CD11b (M1/70), and PECy7-anti-CD4 (RM4-5); PerCpCy5.5-anti-Ly6C (HK1.4), PerCPCy5.5-anti-CD3ε (145-2c11) and PerCPCy5.5-anti-IL17A (1787). The following antibodies were obtained from BD Biosciences: allophycocyanin-anti-CD45.2 (104), FITC-anti-CD44 (IM7), allophycocyanin cy7-anti-Ly6G (IA8), allophycocyanin cy7-anti-CD45.1 (A20), and allophycocyanin cy7-anti-IFNγ (XMG1.2). Rabbit polyclonal antiserum against the amino-terminal ligand binding domain on CXCR2 (MGEFKVDKFNIEDFFSG) was generated by Biosynthesis Inc. as previously described (17, 18). Recombinant mouse (rm)[11]IFNγ and rmIL-12 were from R&D Systems.

Induction and scoring of EAE

Donor mice were immunized subcutaneously with 100μg of peptide $MOG_{35–55}$ (MEVGWYRSP-FSRVVHLYRNGK, Biosynthesis) in CFA (Difco) across four sites over the flanks. Inguinal, axial and brachial lymph nodes were harvested 14 days post-immunization, pooled, homogenized and passed through a 70μm strainer (BD Falcon). Cells were cultured with $MOG_{35–55}$ (50μg/mL) in the presence of rmIL-12 (6ng/mL), rmIFNγ (2ng/mL) and anti-IL-4 mAb (hybridoma 11B11; 10μg/mL). After 96 h, CD4 T cells were isolated by column separation with CD4 (L3T4) magnetic microbeads, according to manufacturer's instructions (Miltenyi). 5×10^6 CD4 T cells (85–99% pure) were transferred i.p. into naïve hosts. Adoptive transfer recipients were monitored on a daily basis by an examiner who was blinded to experimental groups. Mice were scored for severity of conventional and atypical signs of EAE using established scales (14, 19). Specifically, mice with conventional EAE were scored as follows: 0, no abnormality; 1, flaccid tail; 2, waddling gait/ difficulty righting from supine position; 3, overt hindlimb weakness; 4, hindlimb paralysis; 5, forelimb and hindlimb paralysis/moribund. Mice with atypical EAE were scored as follows: 0, no abnormality; 1, slight listing/difficulty righting; 2, obvious imbalance but able to ambulate; 3, severely impaired balance/ambulation; and 4, incapacitated due to inability to maintain upright posture/spinning.

[8]Knock-out (KO)
[9]Myelin Basic Protein (MBP)
[10]Unphosphorylated neurofillament-H (SMI-32)
[11]Recombinant mouse (rm)

Histology

After intracardiac perfusion of mice with 1xPBS and 4% paraformaldehyde (PFA)[12], spinal cords and brainstems were removed. The CNS tissues were then fixed in 4% PFA and cut into 50μm sections on a vibratome (Leica VT1200). Free-floating immunofluorescent staining was performed with primary antibodies against $MBP_{82–87}$ (1:500) and SMI32 (1:1000). Goat anti-mouse IgG AlexaFluor 594 (1:400) and goat anti-rat IgG AlexaFluor 488 (1:1000) were used as secondary antibodies. Sections were incubated with DAPI (100ng/mL) prior to washing and mounting on slides (Prolong Gold anti-fade reagent, Life Technologies). Fluorescent images were acquired with Nikon Eclipse Ti, CoolSnapEZ camera and NIS Elements: Basic Research v3.10. Confocal images were acquired using a Nikon A-1 Confocal microscope (Nikon Plan Fluor 10x/0.30 or Nikon PlanApoVC 60x/1.40 oil) with diode-based laser system and NIS Elements software. 3D reconstruction images were generated with Bitplane software (Imaris) using confocal Z-stack images of equal thickness from each group. Appropriate processing, including image overlays and black level and brightness adjustments, were performed in Adobe Photoshop CS5.1 and applied equally to all samples and controls.

CNS Inflammatory Cell Isolation

CNS tissue was harvested and separated into four compartments: the spinal cord, brainstem, cerebellum and cerebrum. Each tissue was homogenized in 1mL PBS containing a protease inhibitor cocktail (Roche) and centrifuged at 800xg for 10 minutes. Supernatants were stored at −80°C. Tissue pellets were digested with collagenase A (1mg/mL) and DNAse I (1mg/mL) in HBSS containing calcium and magnesium. Inflammatory cells were isolated over a 27/63% percoll gradient and counted with a Cellometer AutoT4 automated cell counter (Nexelcom).

Flow Cytometry

For surface staining, cells were suspended in PBS with 2%FCS containing Fc Block (50ng/mL) prior to incubation with fluorochrome-conjugated antibodies. For intracellular staining, cells were stimulated with PMA (50 ng/ml) and Ionomycin (2 μg/mL) and incubated with Brefeldin A (5 μg/mL) for 6–10 hours. Cells were then fixed in 4% PFA, permeabilized with 0.5% saponin and incubated with fluorochrome-conjugated anti-cytokine antibodies. The stained cells were analyzed with a FACS Canto II flow cytometer using FACSDiva software (v6.1.3, Becton Dickenson). Data was analyzed using FlowJo software (v9.3.2, Treestar).

Multiplex Cytokine Analysis

Cytokine levels in homogenate supernatants were measured via a luminex multiplex bead based assay (Millipore). Data was collected on a Bio-Plex 200 system using the manufacturer's protocols. The data shown indicates levels that fell within the linear portion of a corresponding standard curve. Bradford assays (Thermo Scientific) were performed on tissue homogenates in parallel for normalization to total protein.

[12]Paraformaldehyde (PFA)

Statistical analysis

Statistical analyses were performed using GraphPad Prism software. Two-way ANOVA with Sidak's multiple comparisons test was used to compare disease scores over time. Leukocyte cell numbers and percentages, as well as chemokine and growth factor levels, were compared using the unpaired student's t-test. A P value of <.05 (*) was considered significant. P<0.01 is denoted as (**), P<0.001 as (***).

Results

IFNγR deficiency in host cells increases the incidence of atypical EAE

Following injection with IL-12 polarized $MOG_{35–55}$-specific $CD4^+$ T cells, 44 of 47 WT hosts (94%) and 38 of 48 IFNγRKO hosts (79%) developed clinical EAE. The vast majority of afflicted WT mice had pure conventional disease (31 of 44, or 70%), characterized by an ascending paraparesis with no vestibular signs throughout the clinical course (Table 1, Fig. S1). Of the remainder, 4 (9%) had pure atypical disease (vestibular signs with no evidence of limb weakness) and 9 (21%) exhibited a mixed phenotype, marked by early signs of atypical disease (i.e. a head tilt) that invariably evolved into ascending paraparesis within 1–2 days. None of the WT mice that presented with conventional disease subsequently developed atypical signs. Conversely, the majority of IFNγRKO hosts underwent a pure atypical course (24 of 38, or 62%), while 4 (11%) exhibited a pure conventional, and 10 (26%) a mixed, disease phenotype.

Inflammatory demyelination is prominent in the spinal cord of mice with conventional EAE and in the brainstem of mice with atypical EAE

CNS tissues were collected from representative adoptive transfer recipients at peak disease and sections were examined by immunofluorescent staining. We consistently observed inflammatory infiltration, demyelination and axonopathy of white matter tracts in the spinal cords of WT mice with conventional EAE but not amongst IFNγRKO mice with atypical EAE (Fig. 1, A and B, left panels). In contrast, IFNγRKO mice with atypical EAE displayed pathological changes in white matter surrounding the VCO of the brainstem (Fig. 1A and 1B, right panels). Inflammation of the vestibulocochlear nerve root has also been highlighted in other models of atypical EAE (9, 12, 20). Consistent with these observations, significantly more CNS cells were isolated from the spinal cords of WT hosts at the peak of conventional EAE than from the spinal cords of IFNγRKO hosts at the peak of atypical EAE, while the reverse was true with respect to the numbers of inflammatory cells isolated from the brainstem (Fig. 2A). There were no significant differences between the two cohorts in the number of inflammatory cells isolated from either the cerebral hemispheres or the cerebella.

The severity of atypical EAE correlates with the number of brainstem neutrophils, while the severity of conventional EAE correlates with the number of spinal cord monocytes and donor T cells

We performed a detailed analysis of the cellular composition of leukocytes infiltrating different CNS compartments of IFNγRKO mice that exclusively exhibited signs of atypical

EAE (hereafter referred to as “pure atypical” disease) or of WT mice that exclusively exhibited signs of conventional EAE (hereafter referred to as “pure conventional” disease). Neutrophils comprised a higher percent of total live cells in all CNS compartments of mice with pure atypical EAE when compared to mice with pure conventional EAE (Fig. 2B, left panel). The absolute number of neutrophils was significantly increased in the brainstem, cerebrum and cerebellum of mice with pure atypical disease (Fig. 2B, right panel). In contrast, the percentages and absolute numbers of monocytes/ macrophages and donor T cells were significantly higher in the spinal cords of mice with conventional EAE (Fig. 2C, 2D). The severity of pure atypical disease directly correlated with the number of neutrophils, but not monocytes/ macrophages, infiltrating the brainstem, while the severity of pure conventional EAE directly correlated with the number of monocytes/ macrophages and donor T cells, but not neutrophils, infiltrating the spinal cord (Fig. 2F, 2G, and data not shown). Collectively, the above data suggest that pure atypical EAE is driven by accumulation of neutrophils in the brainstem, and pure conventional EAE is driven by accumulation of monocytes/ macrophages and $CD4^+$ T cells in the spinal cord.

$CD4^+$ donor T cells traffic to the brainstem and upregulate CD25 and CD69 to a similar extent in WT and IFNγRKO hosts during the preclinical phase

EAE lesion formation is initiated several days prior to clinical onset (21, 22). The development of CNS infiltrates is contingent upon the passage of myelin epitope-specific effector T cells across the blood-brain-barrier (BBB)[13] or blood-cerebrospinal fluid barrier (BCSFB)[14] and their reactivation by local antigen presenting cells (23). We questioned whether the distribution of EAE infiltrates in atypical versus conventional EAE reflects differences in trafficking patterns or reactivation of encephalitogenic T cells in the CNS during the preclinical phase. To address that possibility, we adoptively transferred $MOG_{35–55}$-primed, IL-12 polarized $CD4^+$ T cells bearing a CD45.1 congenic marker into $CD45.2^+$ WT and IFNγRKO hosts. Representative mice in each group were euthanized at 1–2 days prior to expected clinical onset and at peak EAE, to analyze CNS infiltrating inflammatory cells by flow cytometry. There was a trend toward a higher number of $CD45.1^+CD4^+$ donor T cells in the brainstem, as well as the spinal cord, of WT compared with IFNγRKO hosts at the preclinical time point (Fig. 3A, 3B). A higher percent of $CD45^{hi}CD11b^+$ cells expressed MHC Class II in WT versus IFNγRKO CNS infiltrates (Fig. 3C), demonstrating the presence of immunocompetent APCs in the brainstem of WT hosts. There were no significant differences between the groups with respect to the number of $CD11b^+CD11c^+$ cells in either the brain or spinal cord (data not shown). The percent of $CD25^+CD69^+$ cells (indicative of recently activated cells) within the $CD44^+$donor T cell population was also comparable between groups (Fig. 3D). Furthermore, we measured similar quantities of IL-2 protein in CNS tissue homogenates from WT and IFNγRKO hosts at clinical onset (data not shown). $CD45.1^+CD4^+$ donor T cells in the brainstem and spinal cord of WT hosts continued to outnumber those cells in IFNγRKO hosts at peak EAE (Fig. 3A, 3B). Collectively, these results led us to conclude that the low incidence of atypical EAE in WT mice could not be attributed to impairment in the early migration of

[13]Blood Brain Barrier (BBB)
[14]Blood Cerebrospinal Fluid Barrier (BCSFB)

encephalitogenic T-cells to the brainstem, or in their reactivation once they had infiltrated the brainstem. However, increased accumulation of donor $CD4^+$ T cells in the spinal cord could be, at least in part, responsible for the enhanced susceptibility of WT hosts to conventional EAE.

Neutrophil attracting chemokines are preferentially upregulated in the brainstem during pure atypical EAE, while monocyte attracting chemokines are preferentially upregulated in the spinal cord during pure conventional EAE

We next focused on events downstream of effector T cell homing and reactivation. The development of clinical signs in EAE coincides with CNS infiltration by a secondary wave of circulating leukocytes, in large part composed of myeloid cells (24). To interrogate the factors that differentially recruit neutrophils to the brainstem of IFNγRKO hosts, and monocytes to the spinal cord of WT hosts, we collected CNS tissue homogenates from representative mice at clinical onset, and measured levels of candidate chemokines. CXCL2, CCL3, and CCL4 were preferentially expressed in brainstem homogenates of IFNγRKO hosts, while CCL2, CCL5, CXCL9 and CXCL10 were expressed at relatively high levels in spinal cord homogenates of WT hosts (Fig. 4). Surprisingly, the neutrophil attracting chemokine CXCL1 was upregulated in the spinal cord and brainstem of WT hosts. The paucity of neutrophils in the CNS infiltrates of WT mice could be secondary to IFNγ-mediated suppression of CXCR2 on neutrophils (25).

IL-12 polarized T cells mediate atypical EAE in IFNγRKO hosts via an IL-17-independent pathway

IL-17 is a potent inducer of CXCL2 (15). In an independent model of EAE induced in the C3H strain, atypical EAE occurs only when Th17 effector cells outnumber Th1 effector cells and is suppressed by IL-17 blockade (11). Although, in our model, donor T cells are polarized with IL-12 and exhibit a classic Th1 profile prior to adoptive transfer (Fig. S3), we entertained the possibility that they upregulate IL-17 themselves, or induce other cell types to produce IL-17, following transfer into IFNγRKO hosts. Therefore, we measured intracellular cytokine levels in CNS infiltrating leukocytes from symptomatic WT and IFNγRKO hosts. A significant percent of transferred $CD45.1^+$ $CD4^+$ donor T cells expressed IFNγ (30–40%) and/ or GM-CSF (17–22%), irrespective of the tissue they had accumulated in, or of host genotype. Conversely, we detected very few IL-17 expressing donor $CD45.1^+$ $CD4^+$ T cells or host $CD45.2^+CD4^+$ T cells in any of the tissues analyzed (< 5%). Consistent with these findings, IFNγ protein was elevated in homogenates of brainstem and spinal cord tissues from WT and IFNγRKO hosts (620–1200 pg/mg), whereas IL-17 was undetectable or expressed at marginal levels (< 5 pg/mg protein). Th2 cytokines (IL-4, IL-5 and IL-13) were also undetectable or at the borderline of detection. To more definitively assess the functional role of IL-17 in our experimental system, we transferred $MOG_{35–55}$-primed, IL-12 polarized donor T cells into IL-17RKO, IFNγRKO or IFNγRKO×IL-17RKO mice. The majority of IL-17R single knock-out mice (63%) developed pure conventional EAE without atypical features (Fig. 5A). IL-17R/IFNγR double knock-out mice exhibited a similar severity and incidence of atypical EAE to IFNγRKO mice (Fig. 5A, and data not shown). Taken together, these experiments demonstrate that, in our experimental paradigm, atypical EAE is IL-17 independent.

CXCR2 blockade abrogates atypical EAE, while CCR2 deficiency abrogates conventional EAE

Based on the chemokine expression patterns shown in Figure 4, we hypothesized that CXCL2 plays an instrumental role in the recruitment of neutrophils to the brainstem of IFNγRKO hosts. However, CCL3 and CCL4 were also induced in the brainstem of IFNγRKO adoptive transfer recipients (Fig. 4), potentially providing a default chemokine pathway for leukocyte recruitment should CXCL2 be blocked. Neutrophils are responsive to a broad array of chemoattractants, including formylated peptides and eicosanoids, that could also function in a redundant manner (26). To directly assess the importance of ELR^+ CXC chemokines in our experimental system, we treated WT and IFNγRKO hosts with anti-sera to CXCR2 (the receptor for CXCL1, CXCL2 and CXCL5) or control sera. Preliminary studies showed that anti-CXCR2 treatment selectively inhibited neutrophil infiltration of the CNS (Fig. S4). CXCR2 blockade abrogated atypical EAE in IFNγRKO hosts, but did not alter the severity of conventional EAE in WT hosts (Fig. 5B). A small percentage of WT hosts treated with control antibody, but none of the WT hosts treated with anti-CXCR2, exhibited atypical signs (data not shown).

The onset of conventional EAE in WT mice is associated with spinal cord expression of the monocyte-attracting CC chemokine CCL2 (Fig. 4). In parallel studies, we transferred $MOG_{35–55}$-primed, IL-12 polarized WT or IFNγKO $CD4^+$ T cells into syngeneic WT or CCR2KO hosts. The severity of conventional EAE was significantly attenuated in CCR2KO compared with WT mice that received WT Th1 cells (Fig. 5C). Conversely, the low incidence of mice that developed atypical features, and the severity of atypical signs, did not differ significantly between the groups. Interestingly, CCR2KO hosts almost exclusively developed atypical EAE following transfer of IFNγKO Th1 donor cells, while WT hosts exhibited a mixture of conventional and atypical features (Fig. 5D).

Discussion

Atypical EAE in IFNγRKO and conventional EAE in WT mice display diametrically different patterns in the spatial distribution of lesions across the neuroaxis. Our data indicate that this is the consequence of distinct CNS region-specific chemokine production following the initial infiltration and reactivation of encephalitogenic T cells. In IFNγRKO mice, CXCL2 is preferentially upregulated in the brainstem. Its cellular source remains to be identified. Astrocytes and choroid epithelial cells are capable of producing ELR^+ CXC chemokines (27–29), which is consistent with the recent observation that IFNγ suppresses atypical EAE via modulation of a non-hematopoietic, radioresistant cell type (10). If brainstem astrocytes are the source of CXCL2, then they might comprise a distinct subset not found in the spinal cord. More definitive conclusions await experiments with IFNγR conditional knockout mice. The factors that induce CXCL2 in the brainstem of IFNγRKO hosts are also unknown. IL-17 was a logical candidate, since it stimulates the production of neutrophil attracting chemokines in a wide variety of cells (15) and has been implicated in alternative models of atypical EAE (11, 14). However, our data demonstrate that atypical EAE induced by the transfer of $MOG_{35–55}$-primed, Th1 polarized WT cells into IFNγRKO hosts is IL-17 independent (Fig. 5). Other candidates include IL-1, TNF α and GM-CSF,

although the levels of those molecules were similar in brainstem and spinal cord homogenates from mice with atypical EAE, and were lower than their respective levels in homogenates from mice with conventional EAE (data not shown).

In WT hosts, CCL2 is upregulated in both the spinal cord and brainstem, but only facilitates parenchymal infiltration of the spinal cord. Donor T cells and monocytes appear to initially cross the BCSFB at the level of the fourth ventricle in WT hosts, but fail to penetrate deep into the brainstem distal to the choroid plexus (Fig.s 1 and 2). This disparity may be the consequence of paradoxical effects of IFNγ-modulated molecules that regulate leukocyte trafficking when expressed in different locations. For example, CXCL12 facilitates neuroinflammation when expressed on the luminal aspect of the cerebrovasculature, but curtails the migration of leukocytes beyond the perivascular space when translocated to the abluminal side (30). IFNγ and IL-17 have opposing effects on the internalization of CXCL12 by brain microvessel endothelial cells. We are currently investigating the effects of IFNγ, produced by encephalitogenic T cells, on the expression of adhesion molecules and chemokines by choroid plexus epithelial cells, glia and cerebrovascular/ meningovascular endothelial cells *in vivo*, and the repercussions for brainstem and spinal cord inflammation.

Lesions are widely distributed throughout the neuroaxis in the majority of MS patients. However, across the spectrum of human demyelinating disease, there are subpopulations in which inflammatory demyelination is consistently focused in a particular region of the CNS, resulting in distinct clinical phenotypes (2, 3, 5, 6). Analogous to atypical and conventional EAE, the pattern of inflammation in human disease tends to associate with particular CNS chemokine profiles and leukocyte subsets. Although EAE does not perfectly simulate MS, the current data illustrates, in principle, how site-specific interactions between infiltrating immune cells and CNS resident cells determine clinical and histopathological phenotypes of autoimmune demyelinating disease. Ultimately, the current line of research might lead to the identification of clinical and radiological features that correlate with CNS immune profiles, thereby facilitating clinical management.

Supplementary Material

Refer to Web version on PubMed Central for supplementary material.

Acknowledgments

Confocal microscopy was performed in the Microscopy and Image-analysis Laboratory (MIL) at the University of Michigan, Biomedical Research Core Facilities (BRCF) with the assistance of MIL Shelley Almburg. The MIL is a multi-user imaging facility supported by NIH-NCI, O'Brien Renal Center, UM Medical School, Endowment for the Basic Sciences (EBS), and the University of Michigan. We would like to thank Lisa Le for assisting with perfusion fixation, vibratome sectioning, and immunofluorescent histology of CNS sections.

References

1. Polman CH, Reingold SC, Banwell B, Clanet M, Cohen JA, Filippi M, Fujihara K, Havrdova E, Hutchinson M, Kappos L, Lublin FD, Montalban X, O'Connor P, Sandberg-Wollheim M, Thompson AJ, Waubant E, Weinshenker B, Wolinsky JS. Diagnostic criteria for multiple sclerosis: 2010 revisions to the McDonald criteria. Ann Neurol. 2011; 69:292–302. [PubMed: 21387374]

2. Ishizu T, Osoegawa M, Mei FJ, Kikuchi H, Tanaka M, Takakura Y, Minohara M, Murai H, Mihara F, Taniwaki T, Kira J. Intrathecal activation of the IL-17/IL-8 axis in opticospinal multiple sclerosis. Brain. 2005; 128:988–1002. [PubMed: 15743872]

3. Rovaris M, Bozzali M, Santuccio G, Ghezzi A, Caputo D, Montanari E, Bertolotto A, Bergamaschi R, Capra R, Mancardi G, Martinelli V, Comi G, Filippi M. In vivo assessment of the brain and cervical cord pathology of patients with primary progressive multiple sclerosis. Brain. 2001; 124:2540–2549. [PubMed: 11701606]

4. Stevenson VL, Leary SM, Losseff NA, Parker GJ, Barker GJ, Husmani Y, Miller DH, Thompson AJ. Spinal cord atrophy and disability in MS: a longitudinal study. Neurology. 1998; 51:234–238. [PubMed: 9674808]

5. Rovaris M, Judica E, Ceccarelli A, Ghezzi A, Martinelli V, Comi G, Filippi M. Absence of diffuse cervical cord tissue damage in early, non-disabling relapsing-remitting MS: a preliminary study. Mult Scler. 2008; 14:853–856. [PubMed: 18611991]

6. Lin X, Blumhardt LD, Constantinescu CS. The relationship of brain and cervical cord volume to disability in clinical subtypes of multiple sclerosis: a three-dimensional MRI study. Acta Neurol Scand. 2003; 108:401–406. [PubMed: 14616292]

7. Raine CS, Barnett LB, Brown A, Behar T, McFarlin DE. Neuropathology of experimental allergic encephalomyelitis in inbred strains of mice. Lab Invest. 1980; 43:150–157. [PubMed: 7401630]

8. Muller DM, Pender MP, Greer JM. Blood-brain barrier disruption and lesion localisation in experimental autoimmune encephalomyelitis with predominant cerebellar and brainstem involvement. J Neuroimmunol. 2005; 160:162–169. [PubMed: 15710469]

9. Abromson-Leeman S, Bronson R, Luo Y, Berman M, Leeman R, Leeman J, Dorf M. T-cell properties determine disease site, clinical presentation, and cellular pathology of experimental autoimmune encephalomyelitis. Am J Pathol. 2004; 165:1519–1533. [PubMed: 15509523]

10. Lee E, Chanamara S, Pleasure D, Soulika AM. IFN-gamma signaling in the central nervous system controls the course of experimental autoimmune encephalomyelitis independently of the localization and composition of inflammatory foci. J Neuroinflammation. 2012; 9:7. [PubMed: 22248039]

11. Stromnes IM, Cerretti LM, Liggitt D, Harris RA, Goverman JM. Differential regulation of central nervous system autoimmunity by T(H)1 and T(H)17 cells. Nat Med. 2008; 14:337–342. [PubMed: 18278054]

12. Lees JR, Golumbek PT, Sim J, Dorsey D, Russell JH. Regional CNS responses to IFN-gamma determine lesion localization patterns during EAE pathogenesis. J Exp Med. 2008; 205:2633–2642. [PubMed: 18852291]

13. Wensky AK, Furtado GC, Marcondes MC, Chen S, Manfra D, Lira SA, Zagzag D, Lafaille JJ. IFN-gamma determines distinct clinical outcomes in autoimmune encephalomyelitis. J Immunol. 2005; 174:1416–1423. [PubMed: 15661899]

14. Kroenke MA, Chensue SW, Segal BM. EAE mediated by a non-IFN-γ/non-IL-17 pathway. Eur J Immunol. 2010; 40:2340–2348. [PubMed: 20540117]

15. Iwakura Y, Ishigame H, Saijo S, Nakae S. Functional specialization of interleukin-17 family members. Immunity. 2011; 34:149–162. [PubMed: 21349428]

16. de Bruin AM, Libregts SF, Valkhof M, Boon L, Touw IP, Nolte MA. IFNγ induces monopoiesis and inhibits neutrophil development during inflammation. Blood. 2012; 119:1543–1554. [PubMed: 22117048]

17. Mehrad B, Strieter RM, Moore TA, Tsai WC, Lira SA, Standiford TJ. CXC chemokine receptor-2 ligands are necessary components of neutrophil-mediated host defense in invasive pulmonary aspergillosis. J Immunol. 1999; 163:6086–6094. [PubMed: 10570298]

18. Hosking MP, Liu L, Ransohoff RM, Lane TE. A protective role for ELR+ chemokines during acute viral encephalomyelitis. PLoS Pathog. 2009; 5:e1000648. [PubMed: 19893623]

19. Kroenke MA, Carlson TJ, Andjelkovic AV, Segal BM. IL-12- and IL-23-modulated T cells induce distinct types of EAE based on histology, CNS chemokine profile, and response to cytokine inhibition. J Exp Med. 2008; 205:1535–1541. [PubMed: 18573909]

20. Muller DM, Pender MP, Greer JM. A neuropathological analysis of experimental autoimmune encephalomyelitis with predominant brain stem and cerebellar involvement and differences

between active and passive induction. Acta Neuropathol. 2000; 100:174–182. [PubMed: 10963365]

21. Skundric DS, Kim C, Tse HY, Raine CS. Homing of T cells to the central nervous system throughout the course of relapsing experimental autoimmune encephalomyelitis in Thy-1 congenic mice. J Neuroimmunol. 1993; 46:113–121. [PubMed: 7689581]
22. Carlson T, Kroenke M, Rao P, Lane TE, Segal B. The Th17-ELR+ CXC chemokine pathway is essential for the development of central nervous system autoimmune disease. J Exp Med. 2008; 205:811–823. [PubMed: 18347102]
23. Kawakami N, Lassmann S, Li Z, Odoardi F, Ritter T, Ziemssen T, Klinkert WE, Ellwart JW, Bradl M, Krivacic K, Lassmann H, Ransohoff RM, Volk HD, Wekerle H, Linington C, Flügel A. The activation status of neuroantigen-specific T cells in the target organ determines the clinical outcome of autoimmune encephalomyelitis. J Exp Med. 2004; 199:185–197. [PubMed: 14734524]
24. Berger T, Weerth S, Kojima K, Linington C, Wekerle H, Lassmann H. Experimental autoimmune encephalomyelitis: the antigen specificity of T lymphocytes determines the topography of lesions in the central and peripheral nervous system. Lab Invest. 1997; 76:355–364. [PubMed: 9121118]
25. Viegas N, Andzinski L, Wu CF, Komoll RM, Gekara N, Dittmar KE, Weiss S, Jablonska J. IFN-γ production by $CD27^+$ NK cells exacerbates Listeria monocytogenes infection in mice by inhibiting granulocyte mobilization. Eur J Immunol. 2013; 43:2626–2637. [PubMed: 23818011]
26. Sadik CD, Kim ND, Luster AD. Neutrophils cascading their way to inflammation. Trends Immunol. 2011; 32:452–460. [PubMed: 21839682]
27. Nygårdas PT, Määttä JA, Hinkkanen AE. Chemokine expression by central nervous system resident cells and infiltrating neutrophils during experimental autoimmune encephalomyelitis in the BALB/c mouse. Eur J Immunol. 2000; 30:1911–1918. [PubMed: 10940880]
28. Glabinski AR, Tani M, Strieter RM, Tuohy VK, Ransohoff RM. Synchronous synthesis of alpha- and beta-chemokines by cells of diverse lineage in the central nervous system of mice with relapses of chronic experimental autoimmune encephalomyelitis. Am J Pathol. 1997; 150:617–630. [PubMed: 9033275]
29. Marques F, Sousa JC, Coppola G, Geschwind DH, Sousa N, Palha JA, Correia-Neves M. The choroid plexus response to a repeated peripheral inflammatory stimulus. BMC Neurosci. 2009; 10:135. [PubMed: 19922669]
30. Cruz-Orengo L, Holman DW, Dorsey D, Zhou L, Zhang P, Wright M, McCandless EE, Patel JR, Luker GD, Littman DR, Russell JH, Klein RS. CXCR7 influences leukocyte entry into the CNS parenchyma by controlling abluminal CXCL12 abundance during autoimmunity. J Exp Med. 2011; 208:327–339. [PubMed: 21300915]

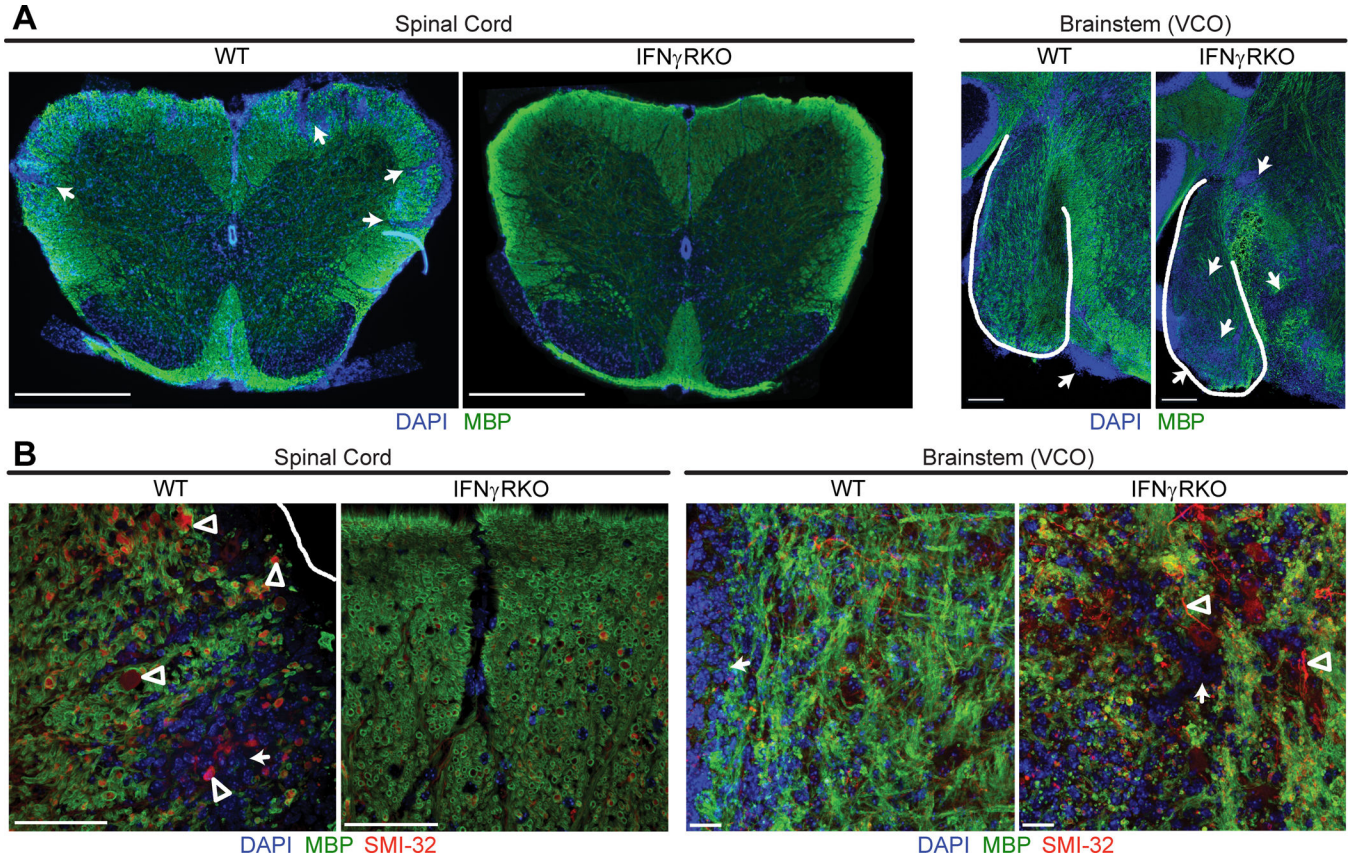

Figure 1.

The distribution of inflammatory demyelination in the CNS of mice with atypical and conventional EAE. (**A**) Representative spinal cord (left) and brainstem (right) sections from WT mice with conventional EAE and IFNγRKO mice with atypical EAE. Sections were stained for MBP (green) and DAPI (blue) to define foci of inflammatory demyelination (arrows). Scale bars are 500 μm in the spinal cord images and 100 μm in the brainstem images. (**B**) Confocal images of spinal cord and brainstem sections stained for MBP (green), SMI-32 (red), and DAPI (blue). Demyelinated axons are SMI-32 positive, MBP negative (arrowheads). Scale bars, 30 μm.

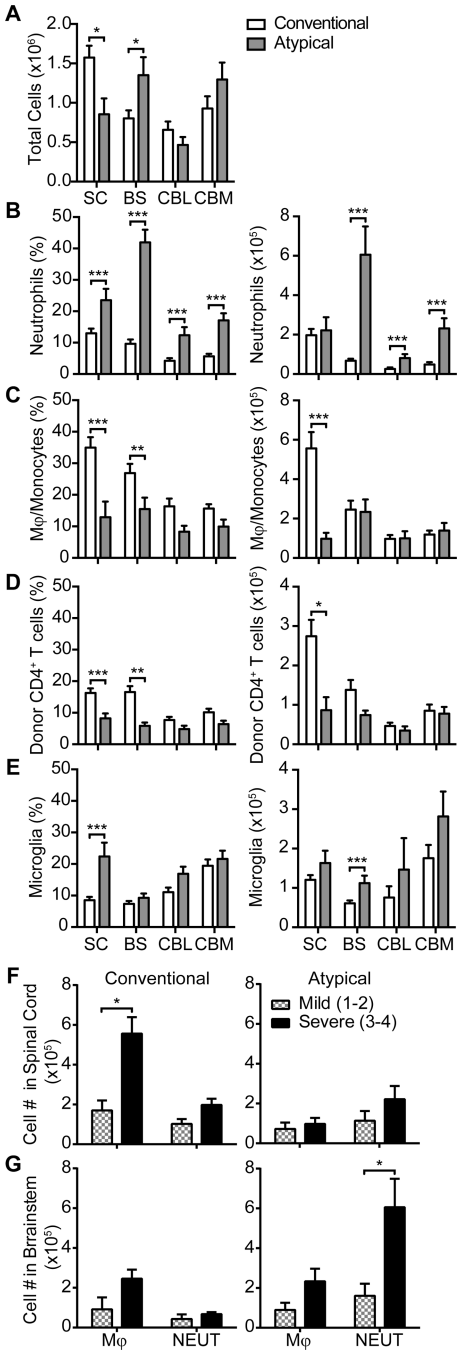

Figure 2.

Neutrophils are prominent in the brainstem of IFNγRO mice with atypical EAE while monocytes and donor T cells are prominent in the spinal cord of WT mice with conventional EAE. (**A**) The average number of total cells isolated from the spinal cord (SC), brainstem (BS), cerebellum (CBL), or cerebrum (CBM) of WT mice with pure conventional and IFNγRO mice with pure atypical EAE. All animals had moderate to severe disease (clinical scores of 3–4) at the time of euthanasia. (**B–E**) Flow cytometry was performed to enumerate the percent and number of infiltrating neutrophils ($CD11b^+CD45^+Ly6G^+$) (**B**), monocytes/

macrophages ($CD11b^{+}CD45^{hi}Ly6G^{-}$) (**C**), donor $CD4^{+}$ T cells ($CD3^{+}CD4^{+}CD45.1^{+}$)(**D**), and microglia ($CD11b^{+}CD45^{int}Ly6G^{-}$) (**E**).

(**F and G**) The absolute number of monocytes (MONO) and neutrophils (NEUT) per spinal cord (**F** and brainstem (**G**) were compared between mice with mild (clinical scores 1–2) or severe (clinical scores 3–4) EAE. Data were pooled from at least 3 experiments with a total of 27 WT and 20 IFNγRKO mice. Flow cytometry gating scheme is illustrated in Fig. S2. *P<.05, **P<.01,***P<.001

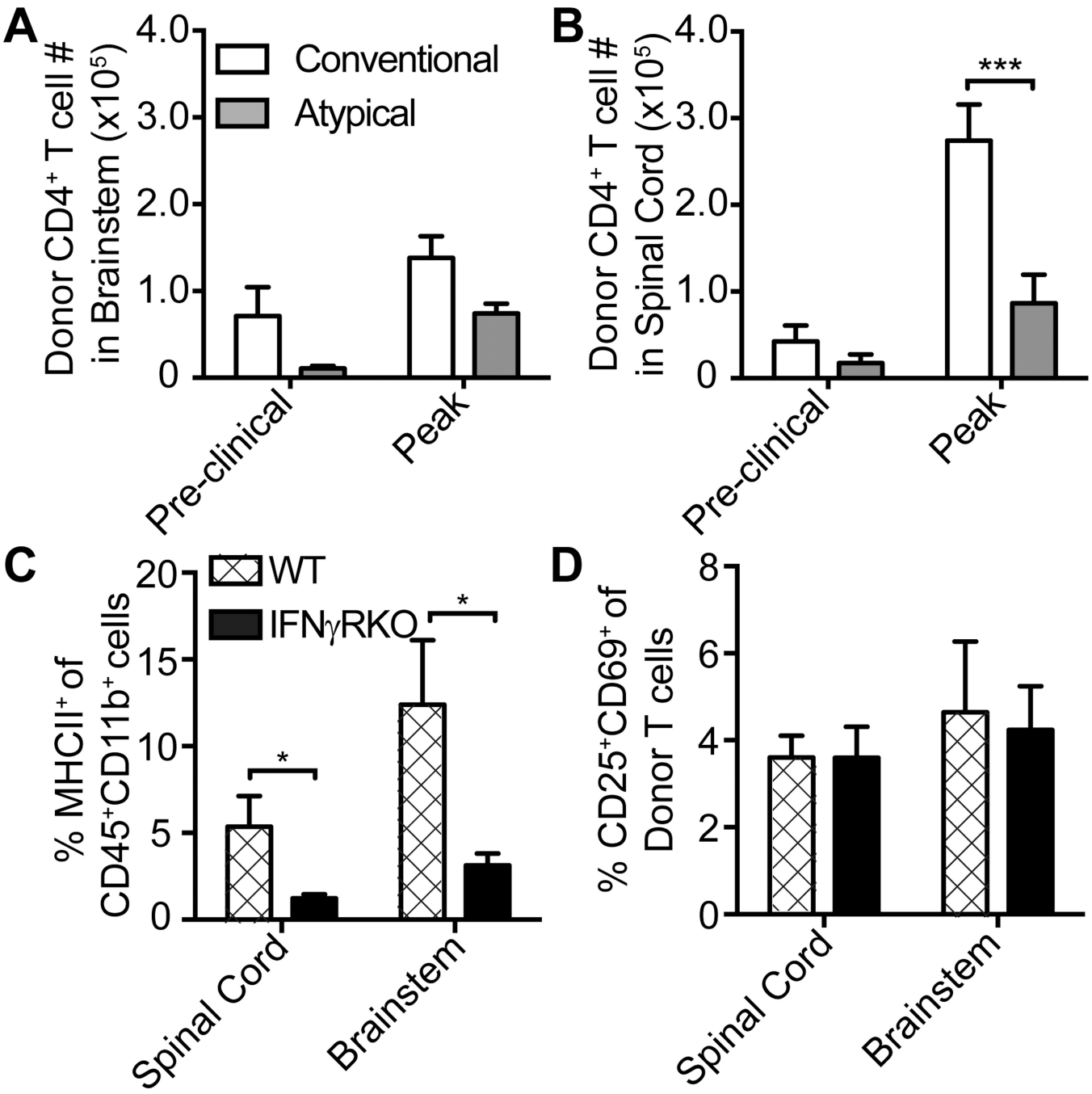

Figure 3.

Enumeration of activated donor $CD4^+$ T cells and antigen presenting cells in the CNS of WT versus IFNγRKO mice. CNS-infiltrating cells were analyzed by flow cytometric analysis. (**A and B**) The average numbers of donor $CD45.1^+$ $CD4^+$ donor T cells ($CD3^+CD4^+CD45.1^+$) the brainstem (**A**) or spinal cord (**B**) of WT and IFNγRKO hosts at preclinical and peak stages of EAE. (**C and D**) Percent of $CD45^+CD11b^+$ that are $MHCII^+$ (**C**) and donor $CD44^+CD4^+$ T cells that are $CD25^+CD69^+$ (**D**) in spinal cord and brainstem of WT and

IFNγRKO at day 6 post-transfer (preclinical time point). The data are representative of three experiments with 3–6 mice per group. *P<.05,***P<.001

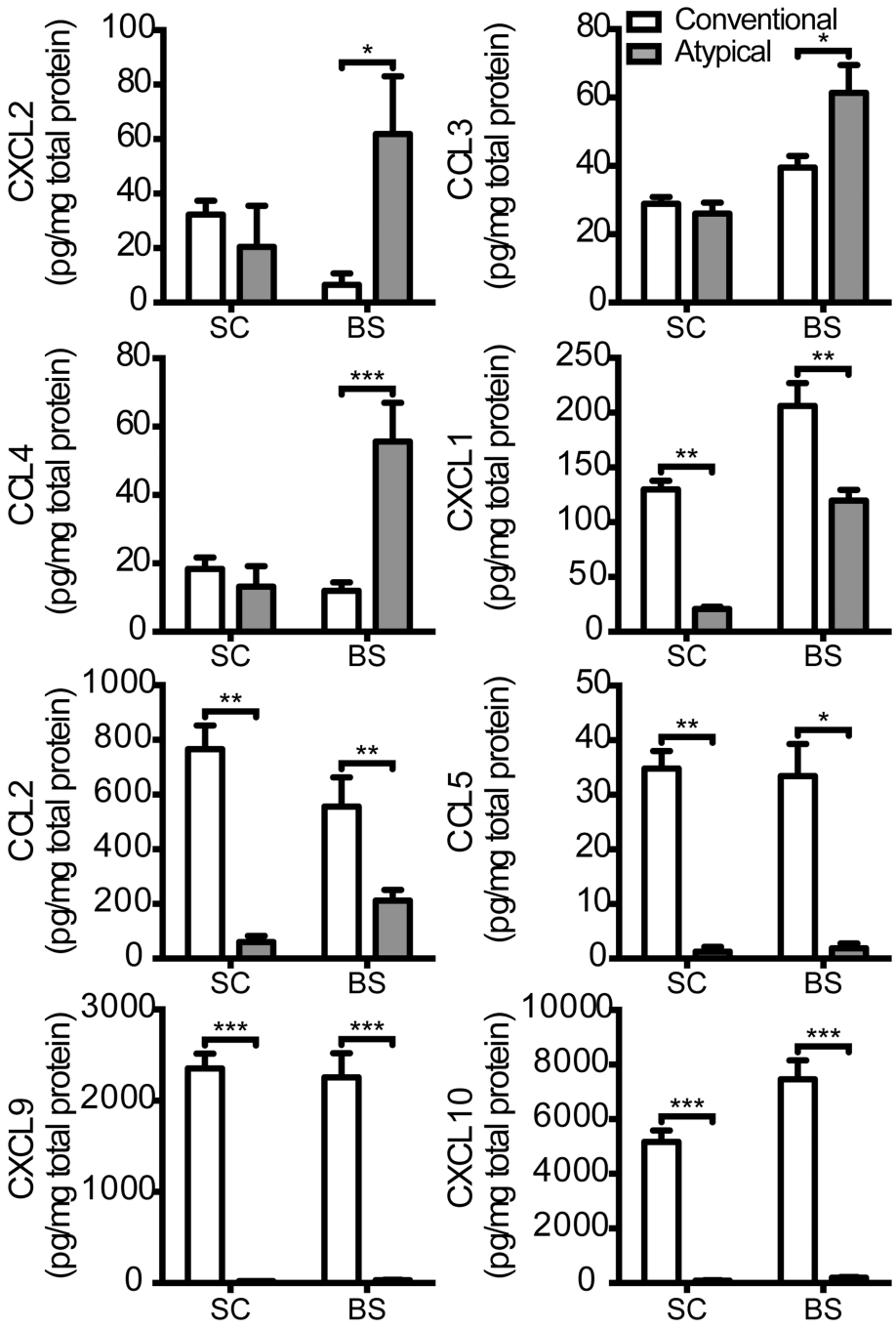

Figure 4.

Chemokine and growth factor expression in the spinal cord and brainstem of mice with pure conventional or pure atypical EAE. Supernatants of spinal cord and brainstem homogenates obtained at clinical onset were subjected to Luminex based multiplex assays to measure levels of a panel of candidate chemokines. Data are pooled from 2 experiments with a total of 6 WT and 8 IFNγRKO mice per group. *P<.05, **P<.01,***P<.001

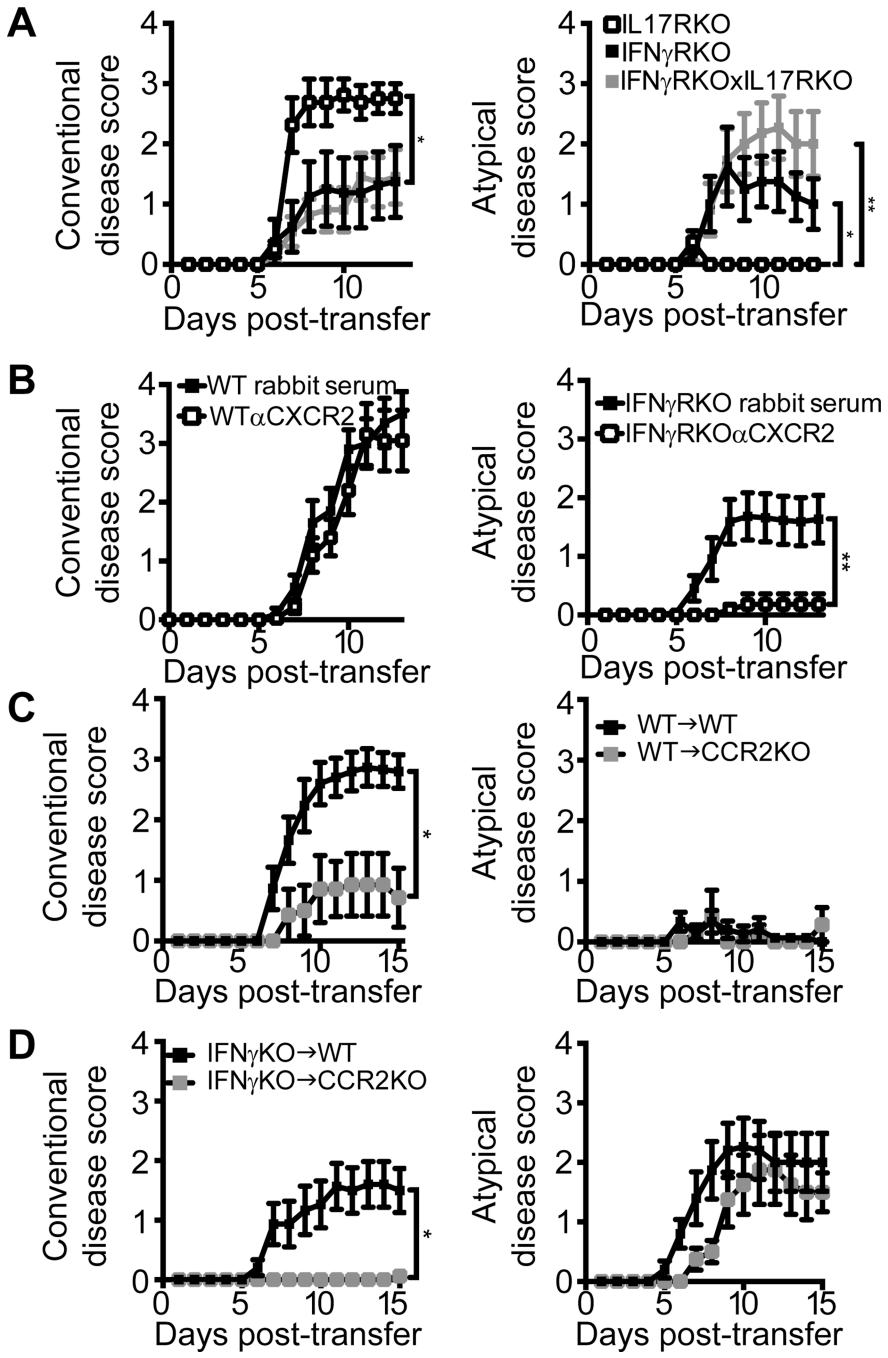

Figure 5.

The pathological role of signature cytokines and chemokines in IFNγRKO and WT adoptive transfer recipients. (**A**) $MOG_{35–55}$ primed, IL-12 polarized $CD4^+$ T cells were transferred into IL-17RKO, IFNγRKO or IFNγRKOxIL-17RKO mice. Data are pooled from two independent experiments with a total of 8 IL-17RKO, 8 IFNγRKO and 11 IL-17RKOxIFNγRKO mice. (**B**) WT and IFNγRKO mice were injected i.p. with α CXCR2 antisera or control rabbit serum on days 0, 2, 4, 6, and 8 following the adoptive transfer of MOG-primed, Th1-polarized $CD4^+$ T cells. Conventional and atypical disease scores were

averaged over 4 experiments with a total of 20–23 mice per group. (**C, D**) WT and CCR2KO mice were injected with $MOG_{35–55}$-primed, Th1-polarized $CD4^+$ WT or IFNγKO T cells and rated for signs of conventional and atypical EAE. WT T cell transfer data are pooled from two representative experiments with 15 WT and 7 CCR2KO recipients. IFNγKO T cell transfer data are from two representative experiments with 15 WT and 9 CCR2KO recipients. The experiment was repeated 4 times with similar results. *P<.05, **P<.01

1Table 1

Conventional and Atypical disease incidence in WT and IFNγRKO recipients of 5×10^6 Th1-polarized $MOG_{35–55}$-reactive CD4 T cells

	EAE Incidence	Disease Phenotype	Incidence
WT	44/47 (93%)	Pure Conventional	31/44 (71%)
		Pure Atypical	4/44 (9%)
		Mixed	9/44 (20%)
IFNγRKO	38/48 (79%)	Pure Conventional	4/38 (10%)
		Pure Atypical	24/38 (63%)
		Mixed	10/38 (27%)

[1] 5×10^6 $MOG_{35–55}$-reactive, Th1-polarized CD4 T cells were purified and transferred into WT and IFNγRKO recipients (as described in the materials and methods). Data were pooled from at least 6 experiments.